Dual-Adaptive Suspension System for Fighter Jet Air-Inlet Inspection Robots

David Meneses*, Sebastian Delour Pacheco Gutierrez, Mayki Mamani Marmillo, Yuri Lester Silva Vidal, and Jorge Luis Apaza Gutierrez

School of Mechanical Engineering, Universidad Nacional de San Agustín de Arequipa, Arequipa, Perú
Email: dmenesesh@unsa.edu.pe (D.M.); spachecog@unsa.edu.pe (S.D.P.G.); mmamanimar@unsa.edu.pe (M.M.M.); ysilvav@unsa.edu.pe (Y.L.S.V.); japazagut@unsa.edu.pe (J.L.A.G.)
*Corresponding author

***Abstract*—This paper compare the locomotion capabilities of the dual adaptability mechanical suspension system, designed for an air intakes inspection robot of a Dassault Mirage 2000P fighter aircraft, with independent suspension coil springs and solid axes suspension systems, which are the most commonly used in wheeled mobile robots for the inspection of pipes, ventilation ducts, tunnels and collapsed buildings, due to their partial similarity to the geometry of the inspection environment. The dual adaptive suspension system is a new mechanism that allows the variation of the relative position of each wheel thanks to two lateral joints that join the two pairs of longitudinal wheels to a central joint that controls the camber. The experimental test in this study evaluate the influence of the suspension on: adaptability, maneuverability, locomotion efficacy, manufacturability and handling complexity. The tests demonstrated technical superiority of 35.6% and 32.9% compared to the Solid Axles system and the Independent Suspension system respectively, proving that it is the most suitable system in environments similar to the air intakes of a fighter aircraft.**

***Keywords*—robot, suspension, curved surfaces, mechanism, mechanical design, inspection robot, variable camber, Suspension, Wheeled Mobile Robots (WMR)**

I. Introduction

In the aeronautical sector, the inspection of the air intakes of an aircraft in the preflight stage is a task dedicated to searching for Foreing Object Debris (FOD) to prevent the risk of its absorption [1, 2]. Currently, the Peruvian Air Force (FAP) has a visual inspection protocol that consists of direct observation through the air intakes for external areas and with a periscope inserted under the aircraft through a slot for internal areas. This protocol has a limited visual range because the periscope fails to provide a clear view to the inspecting technician of the entire surface in the internal area and the inside of the air intake hatches where any FOD could be lodged. Therefore, to reduce the risk of a FOD-related accident during takeoff, a tool that expands the scope of visual inspection in the inner zone is required. To improve this protocol, the FAP aims to implement highly maneuverable Wheeled Mobile Robots (WMR) for inspecting the air intakes of the Mirage 2000P fighter aircraft. These robots must feature integrated locomotion: systems suspension and steering suitable for navigating this environment of smooth surfaces with compound curves, steep slopes, which complicate the proper handling of an inspection WRM. This technology has positioned itself as a safer and more effective alternative for the inspection of confined, narrow and complex geometry environments [3, 4]. For proper implementation, the FAP and the research team have developed a set of technical requirements for suspension and steering:

- Have few parts, and these parts should be easily identified.
- Adapt properly to the geometry of the air intakes by changing the camber and relative position of the wheels.
- Maintain synergy between steering, traction and locomotion mechanisms [5, 6].
- Adequately distribute the loads among all wheels [7, 8].
- Maintain maximum contact points to maintain control during turning maneuvers [9, 10].

According to Gillespie [11] and Jazar [12] mechanical suspension systems are classified into two types according to the dynamic relationship between wheels and vehicle: Solid Axles (SA) and Independent Suspensions (IS). These suspension systems are developed and modified based on the specific characteristics of the locomotion environment. However, in the current air intake environment, the mentioned suspensions are not suitable because they do not meet the requirements and fail to ensure stable movement. Therefore, designing a new suspension system that surpasses them in capabilities is necessary.

The SA suspension is a mechanism that connects two wheels to a rigid component, ensuring a stable position. However, its rigid design limits maneuverability and requires a large amount of space, restricting overall mechanical flexibility [13]. This system has the advantage of being simple and robust and is commonly used in scenarios where complex maneuvers are not required, but considerable traction is needed. Examples

Manuscript received December 23, 2024; revised January 23, 2025; accepted March 6, 2025; published July 4, 2025.

doi: 10.18178/ijmerr.14.4.384-394

include modular robots such as Multi-robot System (MRS), Adaptive Pipe Inspection Robot and Three-plane Pipe Inspection Robot modular robots [14–18] These robots, featuring fixed camber wheels, profiled wheels and wheels distributed at fixed angles attached at various points to a simple SA suspension chassis, have successfully performed thorough visual inspections in demanding and dynamic environments such as internal and external cylindrical surfaces of gas, water, sewage and oil pipelines. However, it is important to note that these robots were designed for one-dimensional trajectory routes with high traction demand and specific inspection routines, which limits their maneuverability. Their adaptability is compromised when encountering significantly larger and more complex obstacles than expected or when facing unexpected changes in their path—scenarios different from those encountered in air intakes. The Independent Suspension Coil Springs (ISCS) system, in contrast, maintains the dynamic independence of each wheel's relative position and camber with respect to the chassis, unlike the SA. This characteristic provides better stability in curves and adaptability to uneven terrain. In locomotion over inclined flat surfaces, obstacles and slightly curved surfaces, this suspension system implemented in robots such as Dune, ROBHAZ-DT3, Hkust, Haulerbot and the Polibot [19–23] slightly adjusts camber and absorb impacts to maintain stability, providing great adaptability. However, these systems generally assume surface irregularities or obstacles in their working path are not large enough to significantly alter their dynamic effectiveness [24–27]. Therefore, for application in air intakes, it is crucial to consider that the geometrically dynamic surface of the inspection area will affect the instantaneous center of rotation and the position/angle of contact between the wheels and the surface.

A hybrid suspension mechanism is proposed, combining characteristics of both suspension types. It utilizes the robustness and design simplicity of SA along with the dynamic maneuverability advantages of IS. Due to the dynamic relationship between lateral and longitudinal wheels, this system is named the Dual Adaptive System (DASS). This system connects the two lateral wheels through a robust central joint that dynamically links the front and rear wheels, as seen in SA suspensions, to properly distribute loads during inclines while maintaining contact points. Additionally, the wheels are interconnected through a central component that controls the independent camber response of each side, adapting to the current curvature during movement and distributing the load efficiently—similar to Independent Suspension systems. Due to the dual dynamic relationship present in all wheels, this suspension features fewer components than ISCS while maintaining flexibility without sacrificing the strength characteristic of SA. It is expected that this system will fulfill the FAP's suspension requirements for WMRs designed for predominantly curved surfaces with steep slopes and obstacles.

The objective of this article is to compare the locomotive capabilities of a WMR equipped with the DASS with those of the Solid Axles (SA) and Independent Suspension Coil Springs (ISCS) systems in locomotion tests for flat surfaces with slopes and cylindrical curved surfaces and in the proposed inspection route for a WMR of the Mirage 2000P fighter aircraft air intake by evaluating their adaptability, maneuverability, efficacy, manufacturability and handling complexity. This study includes the geometrical description of the internal airframe, the mechanical description of the evaluated systems, an experimental analysis of the inspection routes, the analysis of the experimental data and additional comparative data quantifying the evaluation parameters.

II. Work Environment

The variable geometry air intakes on the Dasault Mirage 2000P aircraft are located downstream of the cockpit, in the middle part of the aircraft, their surface is covered with a smooth light-colored metallic material, and they have a "Y" shape on the inside (see Fig. 1(a)). Three points of interest were extracted from the path (see Fig. 1) based on their characteristic geometry or the presence of an obstacle:

- Entry and exit: There are 2 air inlets, located on each side of the cabin, this has the shape of a circular trapezoid as shown in Fig. 1(b) and the minimum space available is 16 cm. This is the area where the robot enters and exits during the inspection.
- Peripheral dampers: The front and rear peripheral dampers are located on either side and are located at the bottom of the air intake, despite being closed in preflight, these have a narrow cavity as seen in Fig. 1(c) and (d).
- Cylindrical intersection: This is the part where the circular trapezoid-shaped air intakes converge in the shape of a circle with a diameter of 78 cm as shown in Fig. 1(c). This area is where the robot changes direction to go to the other intake and finish the inspection.

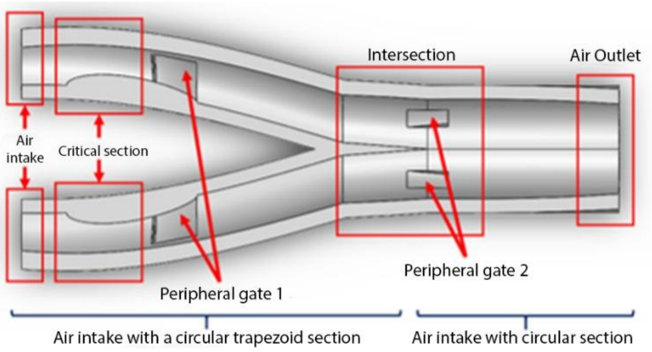

(a)

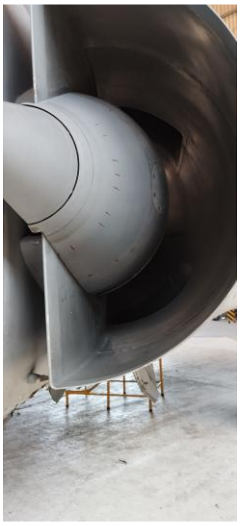

(b)

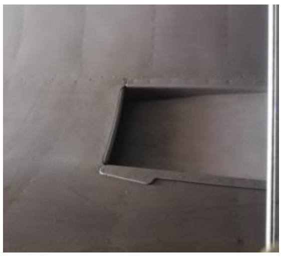

(c)

(d)

(e)

Fig. 1. (a) Inspection route, (b) Inlet and outlet, (c) and (d) Peripheral gates, (e) Cylindrical intersection.

Decomposition of study surfaces:

The inspection route is broken down based on the geometric characteristics of the surface of each zone.

- Flat inclined surface: In the area between the front peripheral hatch and the cylindrical intersection, the curvature is so low that this surface resembles more an inclined plane, however, this area is the one with the steepest slope, so the study surface is an inclined plane with 37° of slope which is the one obtained by the equipment on the aircraft.
- Cylindrical surface: In the area of the cylindrical intersection, the surface is predominantly horizontal cylindrical, so the study surface is a cylinder with a diameter of 78 cm.

III. The Mechanical Characteristics of the Suspension

For a deeper and clearer understanding of the mechanical advantages provided by the DASS suspension system when implemented on a Wheeled Mobile Robot (WMR) designed to operate in inspection environments similar to fighter jet air intakes, two representative suspension systems were developed and analyzed. These systems were selected because they are the most common models in other similar designs and provide a valuable point of comparison for evaluating the performance of the DASS. Two suspension configurations were specifically considered in this study: the Independent Coil Spring Suspension (ISCS) system and the solid axle system (SA), both of which are widely used in various mechanical applications.

A. ISCS Suspension Mechanical Characteristics

The Independent Suspension Coil Springs (ISCS) is a design seen in WMR single wheel all terrain that allows the variation of camber and changes of position of each wheel up or down depending on the contact surface, also this type of suspension keeps a great mechanical and dynamic similarity with the designs seen in automobiles. The WMR with ISCS is 30 cm long. 20 cm wide with standard wheels of 8 cm diameter and 2.5 cm wide, each wheel is driven by a N20 motor that transmits the torque by Cardans printed in PLA material, the suspension consists of 2 coil springs per wheel, the coil spring has the function of maintaining the contact of the wheel with the work surface and changing the value of the camber angle, this amplitude has a maximum of 30°, this robot has a weight of 1 kg. (See Fig. 2(a) and (b)).

B. Mechanical Characteristics of the SA Suspension

The Solid Axles (SA) is a suspension that does not allow the change of the camber or the translation of the wheels, this suspension is considered to be one of the most frequent designs of pipe inspection robots that fix this position in the chassis, in addition, this fixed configuration offers a perspective on the influence of the suspension on the adaptability of a WMR in the path of the air intakes. The WRM with SA is 30 cm long and 15 cm wide, its wheels have a diameter of 6 cm and 3 cm wide, the wheels are connected by a rigid axle that allows the contact of the wheel with the surface, however, these cannot change the camber on the wheel, this robot has a weight of 1.5 kg. (See Fig. 2(c))

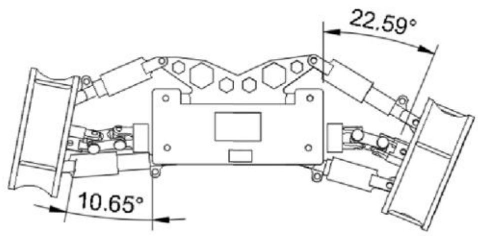

(a)

(b) (c)

Fig. 2. (a) Diagram of ISCS wheel movement, (b) WMR with ISCS suspension, (c) WMR with SA suspension.

C. Mechanical Characteristics of DASS

The Dual Adaptive Suspension System (DASS) is designed to properly adapt the position of the wheels on compound curved surfaces by changing the camber and its relative position with three independent subsystems, a central adaptive system and two lateral suspension systems, these systems are independent of each other, the central suspension is connected to the lateral suspension through the use of a coupling that is positioned in the center of the lateral suspension limiter.

The Double Adaptability Suspension System (DASS) consists of two bearings and four springs, which allow working on flat, convex, concave or geometrically dynamic surfaces. When the surface is convex, the upper springs expand, the lower springs compress, allowing the bearing inside each coupling to change its angular position by a maximum of 15°, generating an angle between the coupling and the bearing support of 75° (see Fig. 3(a)).

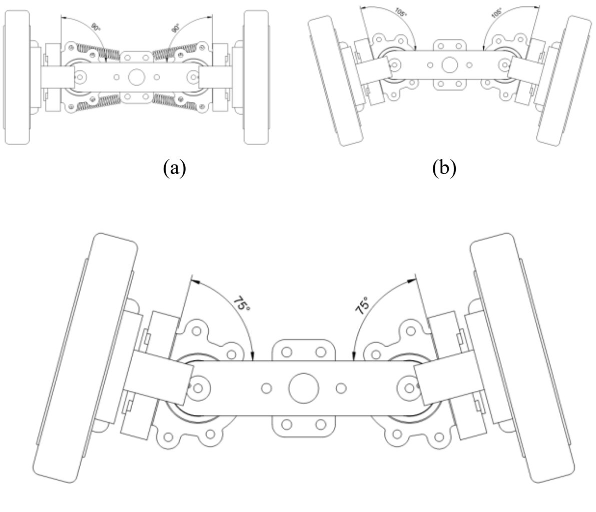

(a) (b)

(c)

Fig. 3. Behavior of the DASS wheels when driving on surfaces (a) Convex, (b) Concave (c) Flat with axis perpendicular to the longitudinal axis of the robot.

On concave surfaces the opposite occurs with respect to convex surfaces, the couplings change their angular position by a maximum of 15° in the opposite direction generating an angle between the coupling and the bearing bracket of 105° (see Fig. 3(b)).

When the surface is flat, the upper and lower springs are at rest, generating an angle 90° between the couplings for the lateral suspension and the bearing support pin (see Fig. 3(c)). As it is an independent system, 9 different combinations can be generated when it is on dynamic geometric surfaces, without considering that they can be at different angles.

The lateral suspension system comprises a limiter, two springs, two bearings, a central axle and two arms that change their amplitude as required, each arm has a bearing at its end, and share the central axle, the central axle is connected in turn with the limiter and the latter with the coupling of the central suspension system, the limiter has at its ends two springs that are joined by a fastener, the movement of the fastener according to the direction of compression of the spring will generate the movement of the arms.

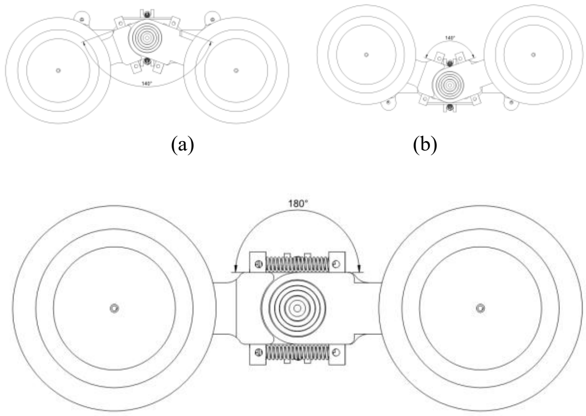

(a) (b)

(c)

Fig. 4. Behavior of the DASS wheels when driving on (a) convex, (b) concave (c) flat surfaces perpendicular to the longitudinal axis of the robot.

When the spring generates a downward force, the arms of the wheels move downwards. This position is ideal for convex surfaces or with the presence of obstacles to overcome, the angular position changes by 20° maximum and generates an angle of 140° between the arms (see Fig. 4(a)), on the other hand, if the surface is similar to the previous one, with cavities or concave, the springs will generate a vertical force with positive sense, this will generate a change of angular position of 20° maximum and an angle of 140° between the arms (see Fig. 4(b)). When the surface is flat, the springs inside the limiter will be at rest, so the angle formed between the wheel arms is 180° (see Fig. 4(c)).

The prototype is designed to work with standard or omnidirectional wheels because of the hexagonal coupling. Each arm has a bearing that is in charge of supporting the axial forces and avoiding breakage due to the separation of layers in the part printed by additive manufacturing, which has a 10% infill with a cubic infill pattern. The prototype consists of a total of 27 parts (see Fig. 5).

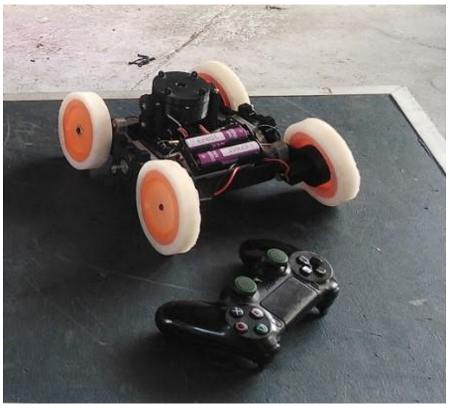

Fig. 5. WMR with DASS suspension.

IV. Experimental Analysis

The experimental analysis is designed to evaluate the effectiveness of the DASS suspension, ISCS, and SA, with the objective of keeping the wheels in perpendicular contact with smooth, curved and geometrically dynamic surfaces, this test protocol was based on the locomotion and mobility tests suggested by the Rescue Robot NIST-ASTM standard. The tests were performed in the air intake of a Mirage 2000 fighter aircraft at the FAP base.

A. *Flat Surface Test*

An inspection robot working on predominantly horizontal and inclined flat terrain generally evaluates its effectiveness by measuring its ability to climb slopes and maneuver without slipping or losing traction from any of the wheels [28–35], therefore, one of the surfaces for the experimental analysis will be that of the inclined plane whose slope value corresponds to the initial angle of curvature that can be found in the air intake of a Mirage 2000P fighter jet.

In this analysis, an inclined flat surface with a slope of 30° was considered the working surface, and the robot had to follow the proposed path (See Fig. 6(a)). The sequence of the path is: A-B-C-C-A-B-D-A, consisting of a straight section (T1), 90° turn (G1), slope ascent (T2), 135° turn (G2), diagonal descent (T3), 45° turn (G3), straight section (T4), 135° turn (G4), diagonal ascent (T5), 45° turn (G5) and slope descent (T6). At each point of the course the ability of the WRM suspension system to maintain wheel contact with the inclined surface (WC) was evaluated, and the Camber Angular value (CA) will not be measured for this test.

Table I shows that: the SA suspension, ISCS, and DASS do not lose contact with the surface at any point, and the coil spring suspension does not manage to make turns without changing position, this is due to the use of standard wheels, and the other two prototypes using omnidirectional wheels are able to perform such movements. With respect to the travel sections, the Solis Axles robot did not manage to make the T3 and T5 by sliding, and due to the presence of small slides in the sections T1 and T4 were not performed optimally.

In the DASS suspension, although at all times the 4 wheels were in contact with the surface (see Fig. 6(b)), changes were observed in the camber with a value of −1°, which is explained by the influence of the turning maneuvers in the behavior of the suspension during the test routes, behavior that is repeated in the other turns presenting similar variations, with this it is inferred that the design of the suspension must consider the influence of the maneuvering mechanism to maintain better stability, in addition, the small variation of the angle indicates that the suspension works better during straight routes with respect to the turns.

Finally, as the suspension kept all four wheels in contact with the surface at acceptable camber angles in both turns and travel, the test is considered a success.

TABLE I. Test (Inclined Plane Test (WC)) Results on Flat Surface Module

Point	SA	ISCS	DASS
A	4	4	4
T1	4	4	4
G1	4	NO TOUR	4
B	4	4	4
T2	4	4	4
G2	4	NO TOUR	4
C	4	4	4
T3	NO TOUR	4	4
G3	4	NO TOUR	4
A	4	4	4
T4	4	4	4
G4	4	NO TOUR	4
B	4	4	4
T5	RESBALA	4	4
G5	4	NO TOUR	4
D	4	4	4
T6	4	4	4
A	4	4	4

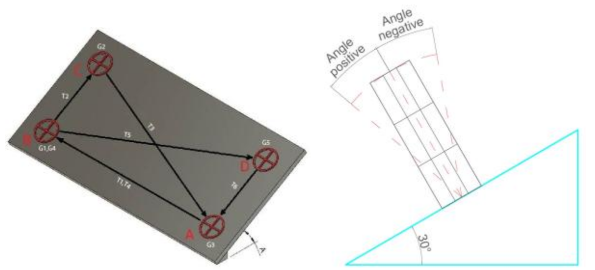

(a) (b)

Fig. 6. (a) Flat surface test module with experimental path arrows, (b) Study angles.

B. *Curved Surface Scaling Test*

A very usual type of route when inspecting confined spaces is those of circular section, for these designs it is considered that the environments in addition to the inclination in the slope have a concave curve of the walls of the pipe with respect to the robot [36–39].

In this test the performance of the suspension system of the robotic prototypes was evaluated when passing through the concave inclined surface located between the intersection and the Z7 of the air intake of the fighter plane, (See Fig. 1(a)), in this case the prototype robots have N20 electric motor reducers with the same capacity and smooth silicone wheels with the same shape, size and weight, so that these do not affect the evaluation of the suspension system.

The sequence of the experimental route is the same as that used in the previous test, (see Fig. 7(a)) is designed to determine the maximum angle of inclination (AE) to which the prototype can climb through a circular curved surface. First, the bearing points of the wheels contacting the surface at various inclinations were evaluated. The maximum inclination was obtained as a consequence of the pressure exerted by the suspension system on the wheels. For this experiment, the radius of the circular section was 700 mm (see Fig. 7(b)) and the static and dynamic coefficient of friction between the wheels and the surface is 0.8 and 0.70 respectively.

Table II shows that the WRM with SA suspension maintains contact at points (A, B) but in the other points only achieves the minimum contact of 2 wheels, for the sections (T1, T4 and T6) are the only ones with a contact of 4 wheels, this is due to the nature of this section, because in more complex sections (T2, T3 and T5) are minimal contact with the surface and especially in sections (T3 and T5) where it slipped and could not obtain the measurement of inclination, T2, T3 and T5) have minimal contact with the surface and especially the sections (T3 and T5) where slipping occurred and the inclination measurement could not be obtained, this type of suspension is not adequate to make the turns either, despite having omnidirectional wheels, when trying to make the turn the wheels lose contact with the surface.

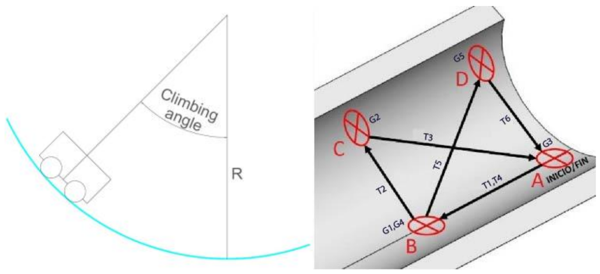

(a) (b)

Fig. 7. (a) Cylindrical surface test module with experimental path arrows, (b) Study angles.

In the Independent Suspension Coil Springs the WRM's 4 wheels remain in contact with the surface in all the control points, it is worth mentioning that at point C the wheels lose contact after making the turn, which is why this value has been considered in Table II. The suspension loses contact up to 2 wheels in the sections (T3, T5) managing to climb and descend with difficulty, in the paths (T1 and T6) the robot maintains the contact of the wheels completely, in the path T6, the robot slips without being able to stop, but it arrives at T2, where the contact is reduced to 3 after the turn. As in the previous suspension, this prototype does not manage to perform the turns on its position.

The DASS system, the wheels are always in contact with the surface at all points, however, as in the suspension mentioned above in point C, it arrives at 4 points of contact, but after making the turn is reduced to 2, during the T2 section at the time of making the turn one of the wheels detached from the study surface, however, this again came into contact at the end of the maneuver. With this we can infer that in curved surfaces the design angles shown in Figs. 4 and 5 should increase the range of movement in future versions to improve the effectiveness during the turning maneuvers, it is also observed that in the highest points of the climbing angle reaches 53°, this means that the suspension has adapted favorably to the surface, also in Sections III and V the number of wheels that came into contact with the surface decreased (2 wheels), which significantly reduced the power and prevented the robot can not turn in position. Another fact to consider is what happened in path 6, the DASS is maintained in the inclined position using an electric brake, but it tends to slip when the electric brake is turned off compared to previous prototypes that fail to maintain in that position, this suggests that a mechanical interlocking system should be implemented in the wheels to remain static on steep inclined surfaces.

In the tests, it was found that the DASS suspension system is superior to the ISCH and SA, however, during the turns of the robot in its position it was not able to execute them easily with standard wheels, due to the low power of the motors and the shape of the wheels which have pronounced edges and jam the robot, this problem could be solved by changing them for omnidirectional wheels. Finally, as the suspension kept all four wheels in contact with the curved surface and an angle greater than 45° was achieved, the test was considered a success.

TABLE II. TEST (INCLINED PLANE TEST (WC)) RESULTS ON CURVED SURFACE MODULUS

Point	SA		ISCS		DASS	
	WC	AE	WC	AE	WC	AE
A	4	3°	4	3°	4	3°
T1	4	3°	4	3°	4	3°
G1	NO TOUR	3°	NO TOUR	3°	4	3°
B	4	3°	4	3°	4	3°
T2	3	25°	4	35°	4	53°
G2	NO TOUR	25°	NO TOUR	35°	4	53°
C	2	25°	4	35°	4	53°
T3	2	RESBALO	4	31°	4	23°
G3	NO TOUR	3°	NO TOUR	3°	4	3°
A	4	3°	4	3°	4	3°
T4	4	3°	4	3°	4	3°
G4	NO TOUR	3°	NO TOUR	3°	4	3°
B	4	-3°	4	3°	4	3°
T5	2	RESBALO	4	14°	4	25°
G5	NO GIRA	23°	NO TOUR	31°	4	47°
D	2	23°	4	31°	4	47°
T6	4	RESBALO	4	RESB ALO	4	47°
A	4	3°	4	3°	4	3°

C. Geometrically Dynamic Surface Test

Finally, when a robot has to work in places where there are several obstacles and unpredictable curves, in addition to slope the surface under the robot is considered geometrically dynamic because more curves and irregularities can appear simultaneously, complicating the locomotion [40–43], however, to evaluate the effectiveness of the mechanism it is also considered that the test surface is a geometrically dynamic one, which in this article are the air intakes of Mirage 2000 fighter jets.

The air intakes are divided into 13 evaluation zones, the tests consist of starting the tour in the right inlet (Z1), crossing the peripheral gates (Z3 and Z6), reaching the cylindrical intersection (Z7) to change to the left side and exit through the same (Z13) (See Fig. 8(a)), as the previous tests, the WC is evaluated for each zone that crosses the WRM, considering that the route starts in the right air intake and ends on the left as shown in Fig. 8(b).

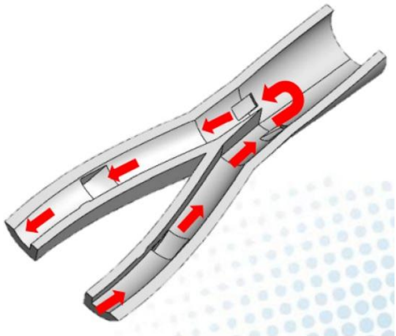

(a)

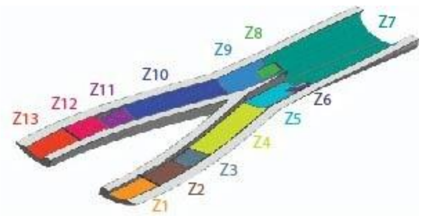

(b)

Fig. 8. Dynamic surface scaling test. (a) 13 study zones. (b) route order.

Table III shows that the WRM with rigid suspension can overcome the zones (Z1, Z2, Z4, Z10, Z12, Z13), however, it was possible to overcome these zones with great difficulty due to the fact that they are 3 WC, these zones could not have angle change in the camber because of the rigid suspension. The zones (Z3, Z5, Z6, Z7, Z8, Z9, Z11) could not be overcome, due to the complexity of the surface, the WRM did not have enough grip so it ended up colliding with the wall of the air intake preventing any movement of the WRM.

The WRM with Independent Suspension Coil Springs did not manage to overcome the zones (Z3 and Z11), which are the ones with the peripheral gates, the WRM is trapped without being able to climb the obstacle, with respect to the zones adjacent to the cylindrical intersection, Z6 and Z8, contact is lost in 2 wheels, 1 front left and 1 rear right, due to the peripheral gate that is located in that zone, however not having great depth if it manages to advance to recover the stability that is lost in the gate. On the camber values all wheels-maintained contact with the surface, however, during the experiment it was noticed that during routes 1 and 3 the suspension had slight inclinations by nature of the route oriented to route 2, forcing one side of the suspension more than the other noticing this effect in the values obtained symmetrical between both routes during this experiment. During route 2 the steering tended to tilt toward low points during the route, however, the suspension adapted adequately at the time of maneuvering to correct the trajectory.

TABLE III. DYNAMIC (DYNAMIC GEOMETRY (WC)) SURFACE MODULUS TEST RESULTS

Point	SA	ISCS	DASS
Z1	3	4	4
Z2	2	4	4
Z3	DOES NOT EXCEED	DOES NOT EXCEED	4
Z4	3	4	4
Z5	DOES NOT EXCEED	4	4
Z6	DOES NOT EXCEED	2	4
Z7	DOES DOES NOT EXCEED	4	4
Z8	DOES DOES NOT EXCEED	2	4
Z9	DOES NOT EXCEED	4	4
Z10	3	4	4
Z11	DOES NOT EXCEED	DOES NOT EXCEED	4
Z12	2	4	4
Z13	3	4	4

The DASS, being a suspension of dynamic adaptation, managed to travel without major effort all the zones of the air intake of the fighter plane maintaining at all times the contact of the wheels with the surface, on the Z7 where is the change of side, this had no complications due to the use of omnidirectional wheels, in areas with peripheral gates such as the Z6 and Z8 zone the prototype managed to overcome these gates without losing its stability, so that the DASS suspension manages to make the journey.

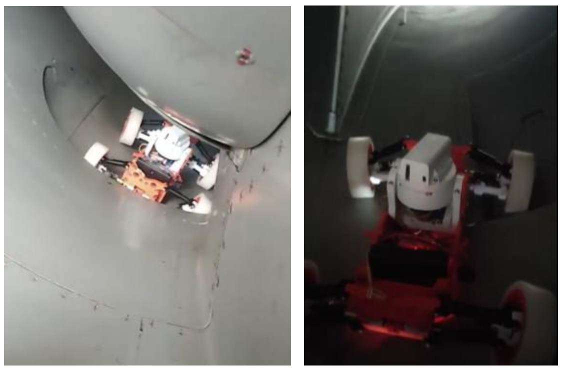

(a) (b)

Fig. 9. WMR of independent suspension coil springs in non-overtopped zones: (a) WMR at peripheral gate Z8, (b) WMR at peripheral gate Z11.

Therefore, it can be concluded that although the Solis Axles suspension is capable of performing 6 of 13 zones, it cannot perform them optimally because it overcomes them with 3 wheels in contact, due to the lack of stability and grip with the surface, in comparison the ISCS presents considerable improvements maintaining greater stability and grip with the surface, The areas that this suspension has not been able to overcome both in outward and return are those with the gates, due to not having a means to climb the obstacle or the power to climb it (see Fig. 9). The DASS suspension improved the results obtained by the two previous prototypes.

V. EVALUATION OF THE DASS PROTOTYPE

Following laboratory and field tests, a selection of quantitative competencies is made, considering areas such as: adaptability, maneuverability, efficacy, manufacturability and complexity. Each of these competencies has indicators with specific scores that allow an accurate comparison between the prototypes.

The adaptability is focused on measuring the capacity of the prototype in question to work on different surfaces (see Fig. 10), which is why for this parameter, we only considered the WC values that each prototype could obtain in the different tests carried out. Table IV shows the values obtained, with a higher DASS score, since the reason for this lies in the score for the air intake travel test. Being the only one with the ability to maintain contact between the wheels and the surface. Although it obtained a higher score than the other prototypes in the curved plane test, it does not obtain the highest score because of the loss of contact in specific movements, it complies with the movement without stopping the test.

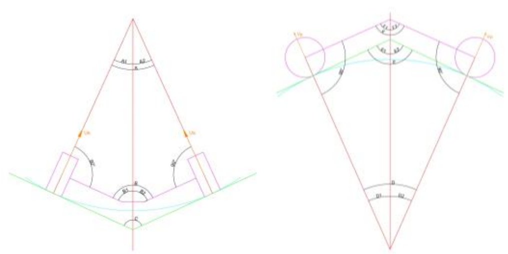

(a) (b)

Fig. 10. Dynamic surface scaling test. (a) Frontal study angle, (b) Lateral study angle.

TABLE IV. PARAMETERIZATION: ADAPTABILITY

INDICATOR	SA	ISCS	DASS
WC according to inclined plane test	17.3	20	20
WC according to the curved plane test	23.04	24.11	25.71
WC according to air intake zones	15.38	38.56	50
Score	55.75	82.57	95.71

Maneuverability focuses on the prototype's ability to make turns and climb obstacles, so the results of the flat and curved surface tests are considered, as well as the maximum slope that the prototype can climb. In Table V, the climbing capacity and the results obtained from the curved surface test are of greater importance, considering a value of 60° of maximum slope, a score was assigned to the prototype. Although the Solis axles did not exhibit good performance, it has had good values in the turning indicators, due to the presence of the omnidirectional wheels. The ISCS has had great deficiencies in the turning areas, only because it has standard wheels and a differential turning system it is not capable of turning without leaving the measuring points, with respect to climbing it surpasses the Solis Axles because it is capable of adapting to the surface improving its traction. The DASS suspension, if it is able to make the turns only because it has omnidirectional wheels, on the climbing capacity it is far above the other two systems despite having the same electromechanical characteristics, resulting in the DASS suspension system being the one with the greatest margin of maneuverability on complex surfaces.

TABLE V. PARAMETERIZATION: MANEUVERABILITY

INDICATOR	SA	ISCS	DASS
Pivots on the inclined plane door	20	0	20
Turns in the curved plane test	0	0	20
Surface scaling capability	25	35	53
Score	45	35	93

With respect to efficacy, this refers to the third test performed, with the objective of quantifying the efficacy of each suspension in the route and overcoming obstacles that may occur in the air intake for which this parameter consists of three indicators, air intake route, overcoming the Z3 and Z11 (presence of peripheral damper) and the turn in the Z7, for each prototype 5 attempts have been made with the aim of seeing the constancy of the suspension system according to the test. In Table VI the null scores of the ER prototype are due to the fact that it did not manage to overcome the obstacle and perform the turn in all the attempts, for the same case the ISCS does not manage to overcome the obstacle, it is for this reason that the DASS is more efficient than the other two systems.

TABLE VI. PARAMETERIZATION: EFFICACY

INDICATOR	SA	ISCS	DASS
Air intake routing	18	24	30
Cold start in zone 3–11	0	0	32
Turn in zone 7	0	24	30
Score	18	48	92

Manufacture and durability is a feature of great importance, for reasons of reliability in the inspection, the prototype cannot fail or suffer breakage of parts inside the air intake, so two indicators have been considered: the number of parts that each prototype has, establishing a maximum of 60 parts between screws, nuts, bearings and components, the value shown in the Table VII is the difference between the maximum number and the total number of parts, the number of parts with breakage after the inspection after the testing,, the parts that were loose or were loose have also been considered as failure, these will subtract one point for failure, for this reason the prototype with fewer components and incidents will be the clear winner. Table VII shows that the ISCS prototype has the lowest score because it has 6 cases of cardan shaft breakage, due to the presence of small components in large quantities, making this system fragile. The prototype with SA has the highest score because it had no cases of breakage and few parts because a rigid chassis protects the internal parts. The prototype with DASS did not achieve the highest score, but its score was similar to the previous prototype, because it had failures in the springs due to breakage of the amplitude limiters. Therefore, for these parameters, it can be concluded that the use of a chassis that protects small and fragile components is of vital importance. Increasing the resistance of the DASS components would improve its score, considering the percentage of filling, the orientation of the piece and applying supports. Although this increases the printing time and the production cost of the prototype, it is essential to obtain better results.

TABLE VII. PARAMETERIZATION: MANUFACTURING

INDICATOR	SA	ISCS	DASS
Number of components	41	7	33
Failure or breakage	50	44	48
Score	91	51	81

Complexity refers to the difficulty of handling and control of the suspension prototype in the path, this parameter takes importance to the opinions of the operator and his sensation of handling in the air intake of the Mirage 2000P fighter plane considering a valuation from 1 to 100 and an importance factor for the path (30 points max), for overcoming obstacles (40 points max) and the turn (30 points max). Table VIII shows that the DASS system gives the best handling sensation in air intake travel, with respect to turning, although the SA and the DASS systems have omnidirectional wheels, the turning was more precise in the DASS because it has better adaptability in the area. Overcoming obstacles is the most important, the best of these three is the DASS, but by only obtaining 20 out of 40, it indicates that although it manages to overcome obstacles, the process is not simple and requires greater effort to achieve it. For this parameter, the parameter that obtained the highest score is the DASS because it has a good driving sensation during both travel, obstacles, and turning. To improve this score it is possible to have a control that allows us to simplify the handling by programing an algorithm that collects the movements used to perform the maneuver.

TABLE VIII. PARAMETERIZATION OF COMPETITIVENESS: COMPLEXITY

INDICATOR	SA	ISCS	DASS
Air intake stroke feel	15	24	27
Control in overcoming obstacles	9	12	20
Rotation control	24	18	27
Score	48	54	74

After comparing all these parameters, the DASS prototype has the best qualities, (see in Fig. 11 and see Table XI), in terms of adaptability, maneuverability, efficacy and complexity.

Although the Solis Axles do not discard in fields such as adaptability, efficacy or complexity, it does improve in maneuverability with respect to the ISCS due to the use of omnidirectional wheels, in size and manufacture it is superior to the other two, due to the low amount of parts and for being quite resistant. For this reason, although the DASS system is a good option for an air intake inspection robot, it still needs to be improved in terms of manufacturing to reduce its components and improve its resistance without affecting its weight. The das system obtained the highest average score, therefore, it is considered the best option for the Mirage200 air intakes route.

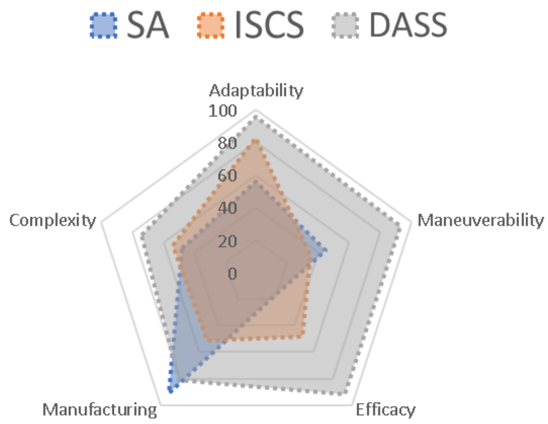

Fig. 11. Suspension comparison.

TABLE IX. SUSPENSION EVALUATION RESULTS

INDICATOR	SA	ISCS	DASS
Adaptability	55.75	82.57	95.71
Maneuverability	45	35	93
Efficacy	18	48	92
Manufacturing	91	51	81
Complexity	48	54	74
Score	51.55	54.15	87.142

VI. CONCLUSION

In this work he develops a WRM with a Dual Adaptive Suspension System (DASS) and analyzes its qualities in air intakes in the aeronautical sector, for the location of Foreing Object Debris (FOD), safety protocol improvements and maintenance.

For this purpose, a performance comparison was made with two other suspension systems, Solid Axles (SA), Independent Suspension Coil Springs (ISCS), we performed tests on Mirage 2000P aircraft on the FAP base, the evaluation parameters are adaptability, maneuverability, efficacy, manufacturability and handling complexity.

It was found that the DASS was superior to the SA suspension by 35.6% and to ISCS by 32.9% in the general results, demonstrating that it was the best in almost all areas. The DASS prototype, with respect to manufacturing, has a score of 81, it is 10% lower than the SA, due to the high number of parts, but it compensates for this with the lower number of failures or breakages. In complexity it surpasses ISCS by 20% for having better handling sensation than other systems, in laboratory and field tests inside the air intake, in adaptability it stands out by 13.1%, in maneuverability it is better by 48% thanks to its climbing capability and omnidirectional wheels, consequently the DASS is more efficient by 42% in travel, it is concluded that the DASS is the WMR type suspension with the best performance on complex surfaces such as the air intakes of a Mirage 2000P fighter jet, however in the performance of the tests we found: the standard wheels of the DASS are inferior to the omnidirectional wheels of the SA for handling in Z7, the implementation of omnidirectional wheels in the DASS improve the performance in maneuverability and handling complexity but reduced it in its manufacturing, causing FOD, the large number of components of the DASS makes it heavy and robust, which complicates its passage in the Z3 and Z11 being occasionally trapped in the cavity of the hatch besides losing at times a Wheel Contac (WC) in the test of curved surface in the T3.

For future work on this suspension system for WMR, we will simplify the mechanism by reducing parts and making them larger so that in case of detachment this can be easily located from the air intakes, we will improve the passage through the Z3 and Z11 zones and simplify the procedure for overcoming these zones, from the experimental analysis it is recommended to increase the limit of the angles for greater adaptability, properly regulate the diameter of the wheels so that the suspension does not come into contact with concave curves and consider the effect of the steering in the operation of the suspension improving the handling control.

Conflict of Interest

The authors declare no conflict of interest.

Author Contributions

P.E.P., Y.L.S., and J.L.A. compiled the requirements; D.M. and S.P. designed the suspension prototypes evaluated; S.P. and M.M.M. developed the tests; D.M. and S.P. wrote the paper; J.L.A. and Y.L.S. obtained the funding. All authors approved the final version.

Funding

This research was funded by Universidad Nacional de San Agustín de Arequipa with contract number IBA-PI-010-2023-UNSA.

Acknowledgment

The authors wish to thank the Universidad Nacional de San Agustín de Arequipa (UNSA), the Fuerza Aérea del Perú (FAP): the 405th Communications Squadron and the 406th Aeronautical Maintenance Squadron of the 4th Air Group, 3rd Air Wing of the Peruvian Air Force for their support in carrying out this work.

References

[1] Y. L. S. Vidal, E. D. S. Colquehuanca, D. F. M. Huanca, E. J. V. Flores, F. J. U. Noa, G. W. G. Alvarez, J. A. G. Mamani, and J. L. A. Gutierrez, "Analysis of robotics applied to mobility in the air intakes of a fighter aircraft," *International Journal of Mechanical Engineering and Robotics Research*, vol. 11, no. 12, 2022.

[2] A. F. El-Sayed, *Foreign Object Debris and Damage in Aviation*, CRC Press, 2022.

[3] K. K. Borkar, T. Aljrees, S. K. Pandey, A. Kumar, M. K. Singh, A. Sinha, K. U. Singh, and V. Sharma, "Stability analysis and navigational techniques of wheeled mobile robot: A review," *Processes*, vol. 11, no. 12, 2023.

[4] A. Verma, A. Kaiwart, N. D. Dubey, F. Naseer, and S. Pradhan, "A 1review on various types of in-pipe inspection robot," *Materials Today: Proceedings*, vol. 50, pp. 1425–1434, 2022.

[5] R. Malekzadeh, *Vehicle Dynamics: Theory and Application*, Cham: Springer, 2021.

[6] Q. Li, K. W. Beyer, and Q. Zheng, "A model-based brake pressure estimation strategy for traction control system," SAE Tech. Paper, 2001.

[7] B. Chol and S. Sreenivasan, "Motion planning of a wheeled mobile robot with slip-free motion capability on a smooth uneven surface," in *Proc. 1998 IEEE Int. Conf. Robot. Autom.*, 1998, vol. 4, pp. 3727–3732.

[8] H.-H. Huang and M.-J. Tsai, "Vehicle cornering performance evaluation and enhancement based on CAE and experimental analyses," *Appl. Sci.*, vol. 9, no. 24, 5428, 2019. doi: 10.3390/app9245428

[9] D. J. Montana, "The kinematics of contact and grasp," *Int. J. Robot. Res.*, vol. 7, no. 3, pp. 17–32, 1988.

[10] J. Shi, X. Li, T. Lu, and J. Zhang, "Development of a new traction control system for vehicles with automatic transmissions," *Int. J. Automot. Technol.*, vol. 13, pp. 743–750, 2012.

[11] T. Gillespie, *Fundamentals of Vehicle Dynamics*, Warrendale, PA, USA: SAE Int., 2021.

[12] R. N. Jazar, *Vehicle Dynamics: Theory and Applications*, New York, NY, USA: Springer, 2008.

[13] W. F. Milliken, D. L. Milliken, and L. D. Metz, *Race Car Vehicle Dynamics*, vol. 400. Warrendale, PA, USA: SAE Int., 1995.

[14] H. Li, Y. Ma, Y. Pan, Y. Xu, and F. Zhao, "Design and development of multirobot system for remote repair of nuclear pipe equipment," Journal of Field Robotics, vol. 41, no. 5, pp. 1297–1312, 2024.

[15] A. A. Bandala *et al.*, "Development of an adaptive pipe inspection robot with rust detection," in *Proc. 2018 IEEE Reg. 10 Symp. (TENSYMP)*, 2018, pp. 271–276.

[16] H. Al-Haboobi, "Calculation and simulation of different speeds of each wheel leg of the wall pressing three-plane pipe inspection robot," in *Proc. 2021 Int. Conf. Commun. Inf. Technol. (ICICT)*, 2021, pp. 62–67.

[17] H. Torajizadeh *et al.*, "Design and manufacturing a novel screw-in-pipe inspection robot with steering capability," *J. Field Robot.*, vol. 40, no. 3, pp. 429–446, 2023. doi: 10.1002/rob.22150

[18] J. M. Mirats Tur and W. Garthwaite, "Robotic devices for water main in-pipe inspection: A survey," *J. Field Robot.*, vol. 27, no. 4, pp. 491–508, 2010.

[19] G. Reina and M. Foglia, "On the mobility of all-terrain rovers," *Ind. Robot Int. J.*, vol. 40, no. 2, pp. 121–131, 2013.

[20] W. Lee *et al.*, "Robhaz-DT3: Teleoperated mobile platform with passively adaptive double-track for hazardous environment applications," in *Proc. 2004 IEEE/RSJ Int. Conf. Intell. Robots Syst. (IROS)*, vol. 1, pp. 33–38, 2004.

[21] A. Pappalettera *et al.*, "Watch the next step: A comprehensive survey of stair-climbing vehicles," *Robotics*, vol. 12, no. 3, 74, 2023. doi: 10.3390/robotics12030074

[22] A. Ugenti *et al.*, "Analysis of an all-terrain tracked robot with innovative suspension system," *Mech. Mach. Theory*, vol. 182, 105237, 2023. doi: 10.1016/j.mechmachtheory.2022.105237

[23] S. R. Thamel *et al.*, "Motion planning of novel stair-climbing wheelchair for elderly and disabled people," in *Proc. 2020 Moratuwa Eng. Res. Conf. (MERCon)*, 2020, pp. 590–595.

[24] R. Siegwart, I. R. Nourbakhsh, and D. Scaramuzza, *Introduction to Autonomous Mobile Robots*, Cambridge, MA, USA: MIT Press, 2011.

[25] R. Rajamani, *Vehicle Dynamics and Control*, New York, NY, USA: Springer, 2011.

[26] S. M. LaValle, *Planning Algorithms*, Cambridge, U.K.: Cambridge Univ. Press, 2006.

[27] J. Auchter and C. A. Moore, "Off-road robot modeling with dextrous manipulation kinematics," in *Proc. 2008 IEEE Int. Conf. Robot. Autom.*, 2008, pp. 2313–2318.

[28] S. Ebrahimi and A. Mardani, "Terramechanics-based performance enhancement of the wide robotic wheel on the soft terrains, part I: Wheel shape optimization," in *Proc. 2017 5th RSI Int. Conf. Robot. Mechatron. (ICRoM)*, 2017, pp. 260–265.

[29] A. Mardani and S. Ebrahimi, "Terramechanics-based performance enhancement of the wide robotic wheel on the soft terrains, part II:

Torque control of the optimized wheel," in *Proc. 2017 5th RSI Int. Conf. Robot. Mechatron. (ICRoM)*, 2017, pp. 480–485.
[30] J. Shen and D. Hong, "Omburo: A novel unicycle robot with active omnidirectional wheel," in *Proc. 2020 IEEE Int. Conf. Robot. Autom. (ICRA)*, 2020, pp. 8237–8243.
[31] C. Ye *et al.*, "Movement performance analysis of mecanum wheeled omnidirectional mobile robot," in *Proc. 2019 IEEE Int. Conf. Mechatron. Autom. (ICMA)*, 2019, pp. 1453–1458.
[32] M. F. A. Jalal, K. S. M. Sahari, and A. Anuar, "Design analysis of boiler header inspection robot MK-02," in *Proc. 2018 Joint 10th Int. Conf. Soft Comput. Intell. Syst. (SCIS) 19th Int. Symp. Adv. Intell. Syst. (ISIS)*, 2018, pp. 683–688.
[33] A. Salunke *et al.*, "Pipe cleaning robot," in *Proc. 2019 Int. Conf. Nascent Technol. Eng. (ICNTE)*, 2019, pp. 1–6.
[34] V. N. Kadam, L. Vachhani, and A. Gupta, "Control of an omnidirectional mobile base with multiple spherical robots," in *Proc. 2019 6th Indian Control Conf. (ICC)*, 2019, pp. 350–355.
[35] A. Papadimitriou *et al.*, "On adhesion modeling and control of a vortex actuator for climbing robots," in *Proc. 2019 IEEE 17th Int. Conf. Ind. Informat. (INDIN)*, 2019, vol. 1, pp. 571–576.
[36] R. Kashyap et al., "Design of reconfigurable in-pipe exploration robots," in *Proc. 2018 Int. Conf. Curr. Trends Towards Converging Technol. (ICCTCT)*, 2018, pp. 1–6.
[37] Y. Wang, X. Li, and F. Yin, "Structural design of a cable climbing robot," in *Proc. 2022 5th World Conf. Mech. Eng. Intell. Manuf. (WCMEIM)*, 2022, pp. 36–40.
[38] Y.-G. Kim *et al.*, "Design and implementation of an optimal in-pipe navigation mechanism for a steel pipe cleaning robot," in *Proc. 2011 8th Int. Conf. Ubiquitous Robots Ambient Intell. (URAI)*, 2011, pp. 772–773.
[39] A. Brusell *et al.*, "Vortex robot platform for autonomous inspection: Modeling and simulation," in *Proc. 2019 45th Annu. Conf. IEEE Ind. Electron. Soc. (IECON)*, vol. 1, pp. 756–762, 2019.
[40] C. Wang, J. Gu, and Z. Li, "Switching motion control of the climbing robot for aircraft skin inspection," in *Proc. 2019 IEEE Int. Conf. Fuzzy Syst. (FUZZ-IEEE)*, 2019, pp. 1–6.
[41] J. Gu and C. Wang, "The adsorption force self-adjustment for the aircraft skin inspection robot with double frames," in *Proc. 2017 36th Chin. Control Conf. (CCC)*, 2017, pp. 6708–6713.
[42] A. Papadimitriou *et al.*, "Development and control of a differential wall climbing robot based on vortex adhesion," in *Proc. 2019 18th Eur. Control Conf. (ECC)*, 2019, pp. 1610–1615.
[43] J. H. Lugo *et al.*, "Conceptual design of tetrad-screw propelled omnidirectional all-terrain mobile robot," in *Proc. 2017 2nd Int. Conf. Control Robot. Eng. (ICCRE)*, 2017, pp. 13–17.